

Split NeissLock with Spy-Acceleration Arms Mammalian Proteins for Anhydride-Mediated Cell Ligation

Sheryl Y. T. Lim,^{||} Anthony H. Keeble,^{||} and Mark R. Howarth*Cite This: *ACS Chem. Biol.* 2025, 20, 2475–2482

Read Online

ACCESS |



Metrics & More

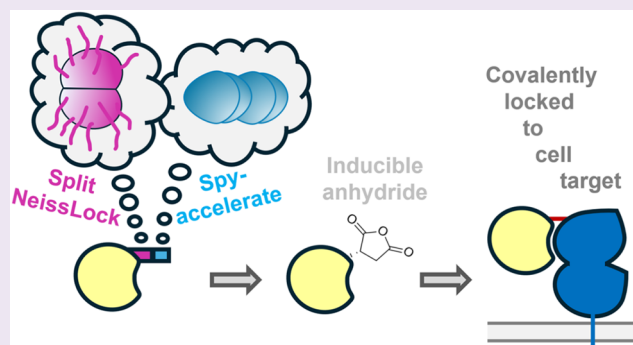


Article Recommendations



Supporting Information

ABSTRACT: Reactive functional groups may be incorporated into proteins or may emerge from natural amino acids in exceptional architectures. Anhydride formation is triggered by calcium in the self-processing module (SPM) of *Neisseria meningitidis* FrpC, which we previously engineered for “NeissLock” ligation to an unmodified target protein. Here, we explored bacterial diversity, discovering a related module with ultrafast anhydride formation. We dissected this swift SPM to generate a split NeissLock system, providing a second layer of control of anhydride generation: first mixing N- and C-terminal NeissLock moieties and second adding millimolar amounts of calcium. Split NeissLock generated a minimal fusion tag, permitting binder expression in mammalian cells with complex post-translational modifications and avoiding self-cleavage while transiting the calcium-rich secretory pathway. Employing spontaneous amidation between SpyTag003 and SpyCatcher003, we dramatically accelerated split NeissLock reconstitution, allowing a rapid high-yield reaction to naturally occurring targets. We established a specific covalent reaction to endogenous Epidermal Growth Factor Receptor using split NeissLock via Transforming Growth Factor- α secreted from mammalian cells. Modular ligation was demonstrated on living cells through site-specific coupling of the clot-busting enzyme tissue plasminogen activator or a computationally designed cytokine. Split NeissLock provides a modular architecture to generate highly reactive functionality, with inducibility and simple genetic encoding for enhanced cellular modification.



INTRODUCTION

Covalent coupling brings new possibilities for robust and long-lasting assemblies, useful for biotransformation,¹ diagnostics,² vaccines,³ and cell therapies.^{4,5} Highly reactive electrophiles such as acid anhydrides and *N*-hydroxysuccinimides are regularly used for coupling to proteins, including for fluorescent labeling and proteomics.^{6,7} Such classic reactants produce broad, uncontrolled reaction.⁶ For covalent coupling to untagged endogenous proteins with more specificity, electrophiles of lower reactivity, such as acrylamide,^{8,9} chloroacetyl,¹⁰ or Sulfur(VI) Fluoride Exchange (SuFEx) probes, are more commonly used.¹¹ Employing these weak electrophiles to direct protein–protein ligation may be limited by the cost and complexity of attaching these electrophiles through a separate reaction (e.g., coupling through cysteine)^{8,9} or through noncanonical amino acid mutagenesis.^{12–14} Hence, we have been exploring ways to incorporate electrophiles into proteins using only the standard 20 amino acids.^{15,16} *Neisseria meningitidis* FrpC contains a self-processing module (SPM) that, upon binding calcium, cleaves at the aspartate-proline (D-P) peptide bond, releasing SPM to reveal an aspartic anhydride (Figure 1A).^{15,16} Aspartic anhydride is a highly reactive electrophile, susceptible to rapid reaction with water.⁶ Developing control of this anhydride's reactivity in diverse

contexts would create new opportunities for molecular engineering.

We previously redirected anhydrides for what we termed NeissLock coupling¹⁷ (Figure 1B), taking advantage of the feature that any protein can be N-terminal to SPM.¹⁶ In NeissLock, a binding protein that interacts noncovalently with a target is fused with SPM (Figure 1B). The two components are then mixed to form a noncovalent complex, before cleavage at aspartate-proline is initiated with calcium. The resulting anhydride can then react with nearby nucleophiles on the target protein, creating an irreversible covalent complex.¹⁷ Here, we enhance the NeissLock system by identifying a faster SPM. We then split the SPM so that NeissLock may be performed on proteins expressed in mammalian cells. Through the use of SpyTag/SpyCatcher, we accelerate the reconstitution of the split SPM system. Then, we demonstrate the

Received: July 3, 2025

Revised: August 11, 2025

Accepted: August 25, 2025

Published: September 15, 2025



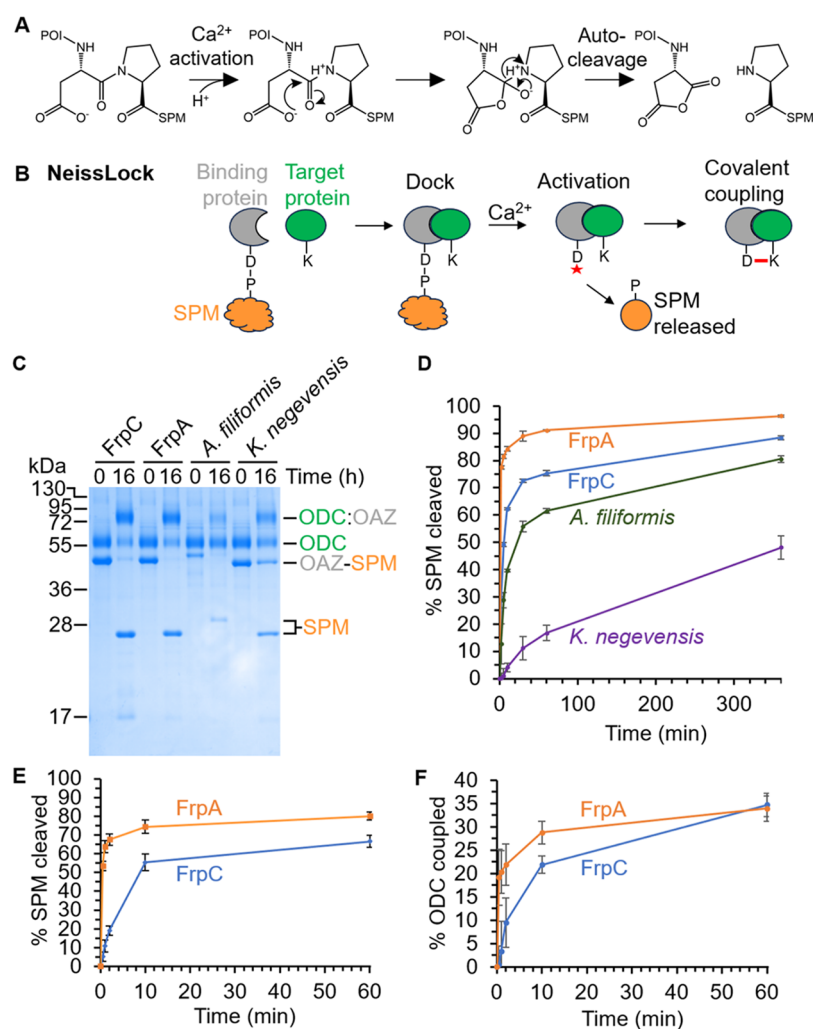


Figure 1. Identifying an ultrafast self-processing module (SPM). (A) SPM undergoes autoproteolysis at Asp-Pro, generating an anhydride. POI is the protein of interest. (B) Schematic of NeissLock. A binding protein genetically fused to SPM docks with a target protein. Upon adding calcium, an anhydride (marked by the red star) is generated on the binding protein, releasing SPM, and enabling covalent coupling to a nucleophile (e.g., lysine, K) on the target. The red line represents an isopeptide bond. (C) Reactivity of SPM homologues. Incubation of different versions of 5 μ M OAZ-SPM with 5 μ M ODC for 0 or 16 h was done with 10 mM calcium at 37 $^{\circ}$ C, before SDS-PAGE/Coomassie analysis. A colon indicates covalent coupling. (D) Time course for SPM cleavage. 5 μ M OAZ-SPM was mixed with 5 μ M ODC for varying times with 10 mM calcium at 37 $^{\circ}$ C, before SDS-PAGE/Coomassie. (E) SPM cleavage rate for FrpA and FrpC with 10 μ M of each partner, after adding 1 mM calcium for the indicated time at 25 $^{\circ}$ C. (F) Coupling rate was tested as in (E). Plots show mean \pm 1 s.d., n = 3.

application of this Spy-accelerated split SPM for covalent ligation of therapeutic proteins to the unmodified Epidermal Growth Factor Receptor (EGFR) at the surface of living cells.

RESULTS

Identification of a Faster Reacting SPM Homologue.

To advance NeissLock chemistry, here our first step was to explore whether other bacterial systems could give superior inducible formation of anhydrides. We bioinformatically identified a panel of SPMs with varying divergence from *N. meningitidis* FrpC (Figure S1). FrpA SPM from *N. meningitidis* shows a 98% amino acid sequence identity to FrpC SPM. SPM of the hemolysin-type calcium-binding protein-related domain-containing protein from *Alysiella filiformis* shows 71% amino acid sequence identity to FrpC. *A. filiformis* is a nonpathogenic bacterium that infects pigs.¹⁸ SPM of the bifunctional hemolysin/adenylate cyclase precursor from *Kingella negevensis* shows 60% amino acid sequence identity to FrpC. *K. negevensis* can be found in the throat of children.¹⁹

As a model for NeissLock coupling, we employed the noncovalent interaction between ornithine decarboxylase (ODC) and ornithine decarboxylase antizyme (OAZ).¹⁷ After calcium activation of NeissLock coupling, previous mass spectrometry (MS) analysis identified K92 as the primary cross-linking site on ODC, with additional cross-linking to other ϵ -amines proximal to the C-terminus of OAZ including K121 and K74.¹⁷ OAZ was genetically fused to the SPM from different species. Each version was efficiently expressed solubly in *Escherichia coli*. All homologues underwent successful calcium-induced cleavage, as well as reaction to the ODC (Figure 1C). FrpA SPM was ultrafast, with $91 \pm 0.2\%$ cleaved after 1 h (Figure 1D, mean \pm 1 s.d., n = 3). The few differences between SPMs of FrpA and FrpC (Figure S2A) have a major effect on the rate. We compared the time course with suboptimal conditions of temperature (25 $^{\circ}$ C) and calcium (1 mM) (Figures S2B and 1E/F). Cleavage and ligation were also substantially faster for FrpA under these conditions. Nearly 70% FrpA SPM was cleaved in 5 min, while FrpC SPM

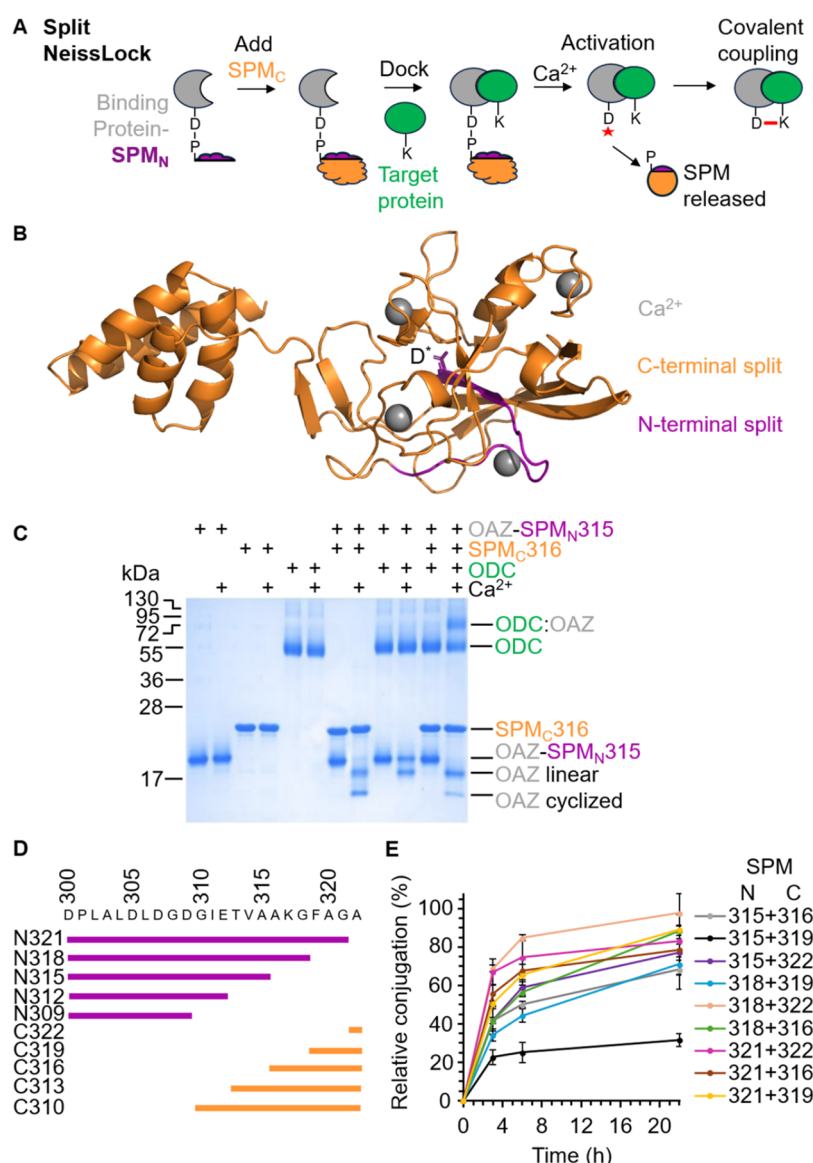


Figure 2. Engineering split NeissLock coupling. (A) Schematic of the split NeissLock. A binding protein genetically fused to the N-terminal fragment of SPM reconstitutes with SPM's C-terminal fragment, before binding the target protein. Calcium activates anhydride generation, promoting ligation to the target. (B) AlphaFold 3 model of FrpA SPM, color-coded for regions for initial splitting into N-terminal (mauve, residues 300 to 315) and C-terminal (orange, residues 316 to 543) fragments. The reactive aspartate (D^*) is shown in a stick format. Ca^{2+} ions are shown as gray spheres. (C) Split NeissLock allows covalent ligation. OAZ-SPM_N315 and SPM_C316 each at 10 μ M were incubated \pm 10 μ M ODC \pm calcium at 37 $^\circ$ C for 16 h, before SDS-PAGE/Coomassie. (D) Schematic of the different tested SPM_N and SPM_C fragments. (E) Time course for ligation using SPM_N and SPM_C fragments. OAZ-SPM_N was premixed with SPM_C, before incubating with ODC (each protein at 5 μ M) along with calcium for the indicated times at 37 $^\circ$ C. Reaction was analyzed by SDS-PAGE/Coomassie (mean \pm 1 s.d., n = 3).

required 60 min or longer to reach the same cleavage extent. Hence, we utilized the ultrafast FrpA SPM for subsequent engineering. Following calcium addition, the two OAZ species of differing mobility on SDS-PAGE (Figure S2B) correspond to a linear species from hydrolysis of the anhydride and a cyclized species from intramolecular reaction of the anhydride with a residue on OAZ itself, as previously validated by MS.¹⁷ There is also potential for reaction of the anhydride with the cleaved SPM, but this side-reaction is likely to be less important since the cleaved SPM will be free to diffuse away from the OAZ-anhydride. It is unclear how frequently the SPM side-reaction with the anhydride occurs, since the product will have the same molecular weight as any OAZ-SPM that fails to be activated.

Engineering a Split SPM to Enable NeissLock Coupling with Mammalian Proteins. It is important for NeissLock to be compatible with binders expressed in the mammalian secretory pathway, since many proteins cannot be functionally expressed in bacteria because of their complex multidomain topology or obligate post-translational modification (e.g., N-linked glycosylation).²⁰ However, we foresaw that the millimolar calcium within the mammalian endoplasmic reticulum during secretion²¹ would likely drive precleavage of SPM.¹⁷ Indeed, when we purified superfolder green fluorescent protein (sfGFP) genetically fused to FrpA SPM, following secretion from human-derived Expi293F cells, a substantial fraction was already cleaved (Figure S3). Aiming to overcome this challenge, we devised a split protein approach, to allow

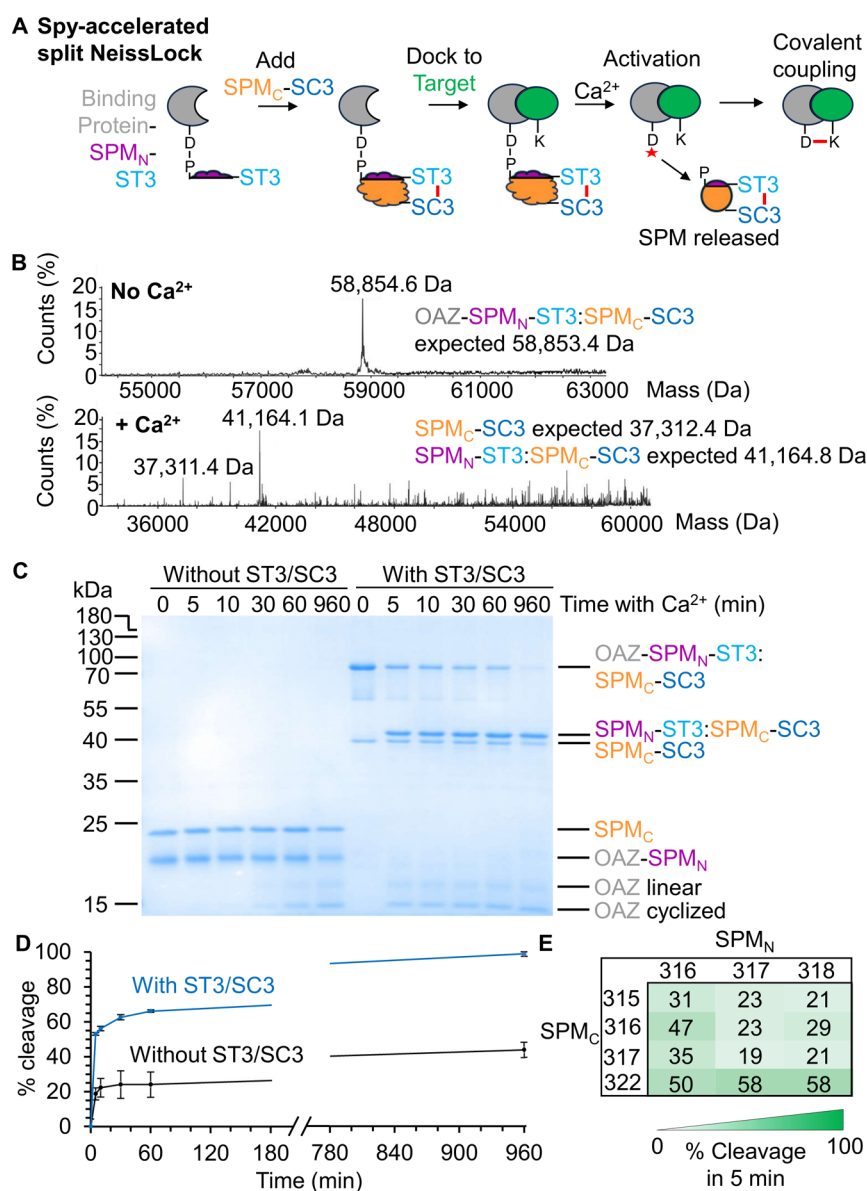


Figure 3. Spy-directed split NeissLock. (A) Schematic of Spy-accelerated split NeissLock. A binding protein fused to SPM's N-terminal fragment and SpyTag003 reacts with SPM's C-terminal fragment fused to SpyCatcher003, to promote SPM reconstitution before calcium activation. (B) Electrospray-ionization MS of reconstitution and SPM cleavage. OAZ-SPM_N-SpyTag003 was incubated with SPM_C-SpyCatcher003 and analyzed \pm calcium. (C) Spy-acceleration of split SPM cleavage. 2 μ M OAZ-SPM_N was incubated with 2 μ M SPM_C \pm SpyTag003/SpyCatcher003 fusion at 37 $^{\circ}$ C, before adding calcium for the indicated time and SDS-PAGE/Coomassie. (D) Quantification of Spy-accelerated cleavage, based on (C) (mean \pm 1 s.d., n = 3). (E) Optimization of the Split Site for Spy-acceleration. Percentage cleavage upon mixing the OAZ-SPM_N-SpyTag003 and SPM_C-SpyCatcher003 variants was displayed as a heat map. 2 μ M of each fragment was preincubated for 1 h at 37 $^{\circ}$ C, before calcium for 5 min (mean of n = 3).

efficient gating of protein function.^{22,23} We designed split FrpA SPM so that NeissLock binding proteins could be expressed with a small inactive N-terminal fragment of SPM (SPM_N) (Figure 2A). Only upon mixing with a C-terminal fragment of SPM (SPM_C) should complete SPM be reconstituted, priming calcium-inducible anhydride generation. We initially split between residues 315 and 316 of FrpA SPM, to give an 18-residue N-terminal fragment, to avoid disrupting the central secondary structure (Figure 2B). The N-terminal portion comprised residues 298 to 315, with the C-terminal portion comprising the rest of the SPM. Indeed, we found calcium-induced cleavage and ligation only upon mixing the two fragments (Figure 2C).

To optimize reconstitution, we varied split positions, and constructs are named after their terminal residue (Figure 2D). Reconstitution was precarious since incubation of SPM_N309 with SPM_C310 or SPM_N312 with SPM_C313 gave no coupling (Figure S4). However, SPM_N318 and SPM_C322 gave excellent reactivity, almost twice that of the original SPM_N315/SPM_C316 (Figure 2E). The location of 318 and 322 within a loop of SPM (Figure 2B) is consistent with studies that splitting within loops is best tolerated.^{22,23} Surprisingly, residues 319–321 are absent from the fastest pair. Hereafter, all experiments were performed with SPM_N318 (N-terminal 298–318; 21 residues) and SPM_C322 (C-terminal 322–543; 222 residues).

has the potential for improving therapeutic efficacy and pharmacokinetics. We selected the well-studied interaction between Transforming Growth Factor- α (TGF α) and EGFR for optimizing split NeissLock coupling to cells. We previously showed that NeissLock could drive covalent ligation of TGF α to EGFR on A431 cells, a human carcinoma cell line.¹⁷ As a model therapeutic to attach, we chose tissue plasminogen activator (tPA), which cleaves plasminogen to plasmin to help degrade fibrin clots as an antithrombotic treatment for stroke²⁵ and myocardial infarction.²⁶ Given the importance of glycosylation of tPA for activity and stability,²⁷ we expressed tPA-TGF α -SPM_N-SpyTag003 in human cells. In this construct, tPA is the model therapeutic, TGF α is the binding protein directing the interaction with EGFR, and SPM_N-SpyTag003 is the module for split NeissLock activation. This multimodule construct was efficiently expressed and purified by SpySwitch chromatography²⁸ (Figure S7), with glycosylation confirmed by Peptide N-Glycosidase F (PNGase F) digestion (Figure S8). For pilot experiments, we first tested coupling to the soluble extracellular region of EGFR (sEGFR). Previously, we showed by MS/MS that NeissLock-activated TGF α reacted with K465 of sEGFR, the closest amine to the C-terminus of TGF α .¹⁷ We employed Spy-directed split FrpA reconstitution and added sEGFR, before activation with calcium. Using the recombinant soluble EGFR ectodomain, we observed the desired formation of the tPA-TGF α -SPM_N-SpyTag003:SPM_C-SpyCatcher003 complex, cleavage to release SPM_N-SpyTag003:SPM_C-SpyCatcher003, and formation of the tPA-TGF α :sEGFR product (Figure 4A).

We next tested coupling to endogenous EGFR at the surface of living human cells. To demonstrate the versatility of the split NeissLock approach, in addition to tPA, we also tested the coupling to cells of a second therapeutic, an interleukin-2 (IL-2) mimetic. IL-2 shows promise as a cancer therapeutic or antiviral, but life-threatening systemic toxicity has limited its use.²⁹ We chose to use the computationally designed Neo2/15 protein that retains high affinity for IL-2 receptor $\beta\gamma_c$ chains, but does not bind IL-2R α or IL-15 α to decrease toxicity.²⁹ Neo2/15 has led to enhanced therapeutic activity in models of melanoma and colon cancer compared to IL-2.²⁹ We genetically fused Neo2/15 to TGF α -SPM_N-SpyTag003, before expression in human cells and purification by SpySwitch chromatography. With split SPM, no precleavage of the Neo2/15 construct was observed during Expi293F expression (Figure S9), whereas the equivalent Neo2/15 construct with full-length SPM was almost completely cleaved by Expi293F cells (Figure S10). After reconstitution of tPA or Neo2/15 linked to TGF α -SPM_N-SpyTag003 with bacterially expressed SPM_C-SpyCatcher003 for 1 h at 25 °C, coupling of tPA or Neo2/15 to A431 cells was activated by the addition of 2 mM calcium. Cells were incubated with the proteins and calcium for 10 min at 37 °C, before subsequent washes to remove unbound proteins. Detecting by anti-TGF α Western blot, only one product band was formed on cells, consistent with the expected molecular weight of tPA or Neo2/15 fused to TGF α :EGFR, illustrating the high specificity of split NeissLock coupling (Figure 4B).

For both tPA and Neo2/15 constructs, the coupling to EGFR was almost completely abolished where hydroxylamine quenched the anhydride (Figure 4B). Hydroxylamine is a strong nucleophile that would outcompete protein nucleophiles in reacting with the cyclic anhydride.¹⁷ This result supports the dependence of coupling on the anhydride

formation. Similarly, mutating the reactive Asp in SPM to Ala (DA) blocked anhydride formation,¹⁷ and consequently, no coupling to EGFR was observed (Figure 4B). Finally, introducing the R42A mutation to TGF α , which disrupts binding to EGFR,³⁰ abolished coupling to EGFR (Figure 4B). This result is consistent with the dependence on initial noncovalent EGFR binding for directing NeissLock-mediated coupling.

DISCUSSION

In summary, we have established unique characteristics of split NeissLock for covalent coupling to living cells, based on 3 advances. First, we identified how the SPM from FrpA provides an ultrafast module for anhydride formation. Second, we showed how an SPM could be dissected into a short peptide and protein partner, creating a new layer of inducibility and enabling eukaryotic expression of complex post-translationally modified building blocks for anhydride-mediated ligation. Third, we established the integration of split NeissLock with the rapid reactivity of SpyTag003/SpyCatcher003. Spy-directed split NeissLock is applicable for specific labeling under cell-compatible conditions within 10 min. Like SPM, SpyTag003/SpyCatcher003 is released from the final complex between the binding protein and the target protein following autoproteolysis. Split NeissLock avoids coupling methodologies involving ultraviolet light or free radical generation,³¹ likely to cause toxicity, and avoids the complexity of noncanonical amino acid mutagenesis.³² We demonstrated modularity by NeissLock coupling with an unmodified cellular receptor using both a therapeutic enzyme and a computationally designed cytokine. There are two regioisomers that can result from attack on a cyclic anhydride, but the regioselectivity in NeissLock is very hard to determine. Previous studies on aspartyl anhydrides showed that attack may occur at either carbonyl, with regioselectivity highly sensitive to solvent polarity and nucleophile identity.³³

Cell therapy is delivering major impact, following clinical successes for CAR-T cells³⁴ and stem cells.³⁵ Although CAR-T cells have been approved for patients with B-cell malignancies or relapsed and/or refractory multiple myeloma, CAR-T cells have shown limited efficacy against most solid tumors, highlighting the need for strategies to enhance CAR-T cell efficacy so that more patients may benefit.³⁶ One such strategy is arming CAR-T cells with cytokines like IL-2 or IL-15 to enhance the potency as well as persistence of CAR-T cells.^{37,38} To do so, CAR-T cells are usually genetically modified to express and secrete immunomodulatory cytokines for local delivery. However, genetic modification adds cost and prolongs the manufacturing time of CAR-T cells. Since it does not require genetic modification, we envision using split NeissLock as a fast and facile way to couple cytokines to CAR-T cells preinfusion. This could improve the CAR-T cell effector function, activate the endogenous immune system, and enhance overall immunotherapy efficacy.

Another possible application of split NeissLock is coupling therapeutic enzymes to red blood cell carriers as circulating bioreactors, capitalizing on the ~120 day circulation time of red blood cells.³⁹ For instance, tPA coupled to red blood cells has potential for treating patients with acute ischemic strokes.⁴⁰ Alternatively, coupling enzymes to red blood cells could help patients with orphan diseases like severe combined immunodeficiency from adenosine deaminase deficiency,⁴¹ or Mitochondrial Neurogastrointestinal Encephalomyopathy

(MNGIE) from thymidine phosphorylase deficiency.⁴² Currently, patients with metabolic deficiencies require regular intravenous enzyme replacement therapy infusions. By coupling enzymes to red blood cells, the frequency of the infusions could be reduced. Currently, few methods are available to modify the surface of red blood cells while preserving red blood cell function.^{39,43} Split NeissLock could be used to engineer red blood cells to carry therapeutic enzymes with minimal impact on the integrity of the plasma membrane. All in all, it is vital to advance the engineering of highly reactive proteins like split NeissLock to fulfill the potential of modular cell decoration.

■ ASSOCIATED CONTENT

SI Supporting Information

The Supporting Information is available free of charge at <https://pubs.acs.org/doi/10.1021/acschembio.5c00515>.

Additional materials and methods; amino acid alignment of SPM homologs; and amino acid sequences of finalized split NeissLock pair compared to parental FrpA SPM (PDF)

■ AUTHOR INFORMATION

Corresponding Author

Mark R. Howarth – Department of Biochemistry, University of Oxford, Oxford OX1 3QU, U.K.; Department of Pharmacology, University of Cambridge, Cambridge CB2 1PD, U.K.; orcid.org/0000-0001-8870-7147; Email: mh2186@cam.ac.uk

Authors

Sheryl Y. T. Lim – Department of Biochemistry, University of Oxford, Oxford OX1 3QU, U.K.; Present Address: Institute of Molecular and Cell Biology, Agency for Science, Technology and Research (A*STAR), 61 Biopolis Drive, Singapore 138673, Singapore; orcid.org/0000-0002-2606-9220

Anthony H. Keeble – Department of Pharmacology, University of Cambridge, Cambridge CB2 1PD, U.K.

Complete contact information is available at:

<https://pubs.acs.org/doi/10.1021/acschembio.5c00515>

Author Contributions

[§]S.Y.T.L. and A.H.K. contributed equally to this work.

Notes

The authors declare the following competing financial interest(s): S.Y.T.L. and M.R.H. are authors on a patent application covering sequences for anhydride formation (UK Intellectual Property Office Patent Application No. 2504781.2). S.Y.T.L. and M.R.H. are authors on a patent application covering NeissLock (UK Intellectual Property Office Patent Application No. 2003683.6). A.H.K. and M.R.H. are authors on patents covering sequences for enhanced isopeptide bond formation (UK Intellectual Property Office 1706430.4 and 1903479.2).

■ ACKNOWLEDGMENTS

S.Y.T.L. was funded by an A*STAR studentship. We thank Dr. Anthony Tumber of the University of Oxford Department of Chemistry for help with MS, through support from the Biotechnology and Biological Sciences Research Council (BBSRC, grant BB/R000344/1). A.H.K. and M.R.H. were

funded by the Engineering and Physical Sciences Research Council (EPSRC EP/T030704/1).

■ REFERENCES

- (1) Peschke, T.; Bitterwolf, P.; Gallus, S.; Hu, Y.; Oelschlaeger, C.; Willenbacher, N.; Rabe, K. S.; Niemeyer, C. M. Self-Assembling All-Enzyme Hydrogels for Flow Biocatalysis. *Angew. Chem., Int. Ed.* **2018**, *57*, 17028–17032.
- (2) Squires, T. M.; Messinger, R. J.; Manalis, S. R. Making It Stick: Convection, Reaction and Diffusion in Surface-Based Biosensors. *Nat. Biotechnol.* **2008**, *26*, 417–426.
- (3) Hills, R. A.; Howarth, M. Virus-like Particles against Infectious Disease and Cancer: Guidance for the Nano-Architect. *Curr. Opin. Biotechnol.* **2022**, *73*, 346–354.
- (4) Minutolo, N. G.; Sharma, P.; Poussin, M.; Shaw, L. C.; Brown, D. P.; Hollander, E. E.; Smole, A.; Rodriguez-Garcia, A.; Hui, J. Z.; Zappala, F.; Tsourkas, A.; Powell, D. J., Jr. Quantitative Control of Gene-Engineered T-Cell Activity through the Covalent Attachment of Targeting Ligands to a Universal Immune Receptor. *J. Am. Chem. Soc.* **2020**, *142* (14), 6554–6568.
- (5) Shi, Y.; Bashian, E. E.; Hou, Y.; Wu, P. Chemical Immunology: Recent Advances in Tool Development and Applications. *Cell Chem. Biol.* **2024**, *31* (3), 387–408.
- (6) Spanedda, M. V.; Bourel-Bonnet, L. Cyclic Anhydrides as Powerful Tools for Bioconjugation and Smart Delivery. *Bioconjugate Chem.* **2021**, *32* (3), 482–496.
- (7) Wang, Z.; Liu, P. K.; Li, L. A Tutorial Review of Labeling Methods in Mass Spectrometry-Based Quantitative Proteomics. *ACS Meas. Sci. Au.* **2024**, *4* (4), 315–337.
- (8) Holm, L.; Moody, P.; Howarth, M. Electrophilic Affibodies Forming Covalent Bonds to Protein Targets. *J. Biol. Chem.* **2009**, *284*, 32906–32913.
- (9) Chmura, A. J.; Orton, M. S.; Meares, C. F. Antibodies with Infinite Affinity. *Proc. Natl. Acad. Sci. U.S.A.* **2001**, *98*, 8480–8484.
- (10) Qiu, J.; Nie, Y.; Zhao, Y.; Zhang, Y.; Li, L.; Wang, R.; Wang, M.; Chen, S.; Wang, J.; Li, Y.-Q.; Xia, J. Safeguarding Intestine Cells against Enteropathogenic *Escherichia Coli* by Intracellular Protein Reaction, a Preventive Antibacterial Mechanism. *Proc. Natl. Acad. Sci. U.S.A.* **2020**, *117* (10), 5260–5268.
- (11) Liu, J.; Yang, B.; Wang, L. Residue Selective Crosslinking of Proteins through Photoactivatable or Proximity-Enabled Reactivity. *Curr. Opin. Chem. Biol.* **2023**, *74*, No. 102285.
- (12) Zhang, H.; Han, Y.; Yang, Y.; Lin, F.; Li, K.; Kong, L.; Liu, H.; Dang, Y.; Lin, J.; Chen, P. R. Covalently Engineered Nanobody Chimeras for Targeted Membrane Protein Degradation. *J. Am. Chem. Soc.* **2021**, *143* (40), 16377–16382.
- (13) Xuan, W.; Li, J.; Luo, X.; Schultz, P. G. Genetic Incorporation of a Reactive Isothiocyanate Group into Proteins. *Angew. Chem., Int. Ed.* **2016**, *55* (34), 10065–10068.
- (14) Wang, N.; Yang, B.; Fu, C.; Zhu, H.; Zheng, F.; Kobayashi, T.; Liu, J.; Li, S.; Ma, C.; Wang, P. G.; Wang, Q.; Wang, L. Genetically Encoding Fluorosulfate-l-tyrosine To React with Lysine, Histidine, and Tyrosine via SuFEx in Proteins in Vivo. *J. Am. Chem. Soc.* **2018**, *140* (15), 4995–4999.
- (15) Osicka, R.; Prochazkova, K.; Sulc, M.; Linhartova, I.; Havlicek, V.; Sebo, P. A Novel “Clip-and-Link” Activity of Repeat in Toxin (RTX) Proteins from Gram-Negative Pathogens. *J. Biol. Chem.* **2004**, *279*, 24944–24956.
- (16) Sadilkova, L.; Osicka, R.; Sulc, M.; Linhartova, I.; Novak, P.; Sebo, P. Single-Step Affinity Purification of Recombinant Proteins Using a Self-Excising Module from *Neisseria Meningitidis* FrpC. *Protein Sci.* **2008**, *17*, 1834–1843.
- (17) Scheu, A. H. A.; Lim, S. Y. T.; Metzner, F. J.; Mohammed, S.; Howarth, M. NeissLock Provides an Inducible Protein Anhydride for Covalent Targeting of Endogenous Proteins. *Nat. Commun.* **2021**, *12*, No. 717.
- (18) Zutic, J.; Radosavljevic, V.; Radanovic, O.; Ivetic, V.; Pavlovic, I.; Zutic, M. A Case Report: Isolation of *Alysiella Filiformis* from Pig's Lungs. *Kafkas Univ. Vet. Fak. Derg.* **2013**, *19* (4), 721–723.

- (19) Yagupsky, P.; El Houmami, N.; Fournier, P.-E. Respiratory Carriage of the Novel *Kingella Negevensis* Species by Young Children. *New Microbes New Infect.* **2018**, *26*, 59–62.
- (20) Schütz, A.; Bernhard, F.; Berrow, N.; Buyel, J. F.; Ferreira-da-Silva, F.; Haustraete, J.; van den Heuvel, J.; Hoffmann, J.-E.; de Marco, A.; Peleg, Y.; Suppmann, S.; Unger, T.; Vanhoucke, M.; Witt, S.; Remans, K. A Concise Guide to Choosing Suitable Gene Expression Systems for Recombinant Protein Production. *STAR Protocols* **2023**, *4* (4), No. 102572.
- (21) Mekahli, D.; Bultynck, G.; Parys, J. B.; De Smedt, H.; Missiaen, L. Endoplasmic-Reticulum Calcium Depletion and Disease. *Cold Spring Harbor Perspect. Biol.* **2011**, *3* (6), No. a004317.
- (22) Dagliyan, O.; Krokhotin, A.; Ozkan-Dagliyan, I.; Deiters, A.; Der, C. J.; Hahn, K. M.; Dokholyan, N. V. Computational Design of Chemogenetic and Optogenetic Split Proteins. *Nat. Commun.* **2018**, *9* (1), No. 4042.
- (23) Anastassov, S.; Filo, M.; Khammash, M. Inteins: A Swiss Army Knife for Synthetic Biology. *Biotechnol. Adv.* **2024**, *73*, No. 108349.
- (24) Keeble, A. H.; Turkki, P.; Stokes, S.; Anuar, I. N. A. K.; Rahikainen, R.; Hytonen, V. P.; Howarth, M. Approaching Infinite Affinity through Engineering of Peptide-Protein Interaction. *Proc. Natl. Acad. Sci. U.S.A.* **2019**, *116*, 26523–26533.
- (25) Zhu, A.; Rajendram, P.; Tseng, E.; Coutts, S. B.; Yu, A. Y. X. Alteplase or Tenecteplase for Thrombolysis in Ischemic Stroke: An Illustrated Review. *Res. Pract. Thromb. Haemostasis* **2022**, *6* (6), No. e12795.
- (26) Guillermin, A.; Yan, D. J.; Perrier, A.; Marti, C. Safety and Efficacy of Tenecteplase versus Alteplase in Acute Coronary Syndrome: A Systematic Review and Meta-Analysis of Randomized Trials. *Arch. Med. Sci.* **2016**, *6*, 1181–1187.
- (27) Toul, M.; Slonkova, V.; Mican, J.; Urminsky, A.; Tomkova, M.; Sedlak, E.; Bednar, D.; Damborsky, J.; Herynychova, L.; Prokop, Z. Identification, Characterization, and Engineering of Glycosylation in Thrombolytics. *Biotechnol. Adv.* **2023**, *66*, No. 108174.
- (28) Vester, S. K.; Rahikainen, R.; Khairil Anuar, I. N. A.; Hills, R. A.; Tan, T. K.; Howarth, M. SpySwitch Enables pH- or Heat-Responsive Capture and Release for Plug-and-Display Nanoassembly. *Nat. Commun.* **2022**, *13* (1), No. 3714.
- (29) Silva, D.-A.; Yu, S.; Ulge, U. Y.; Spangler, J. B.; Jude, K. M.; Labão-Almeida, C.; Ali, L. R.; Quijano-Rubio, A.; Ruterbusch, M.; Leung, I.; Biary, T.; Crowley, S. J.; Marcos, E.; Walkey, C. D.; Weitzner, B. D.; Pardo-Avila, F.; Castellanos, J.; Carter, L.; Stewart, L.; Riddell, S. R.; Pepper, M.; Bernardes, G. J. L.; Dougan, M.; Garcia, K. C.; Baker, D. De Novo Design of Potent and Selective Mimics of IL-2 and IL-15. *Nature* **2019**, *565* (7738), 186–191.
- (30) Lazar, E.; Vicenzi, E.; Van Obberghen-Schilling, E.; Wolff, B.; Dalton, S.; Watanabe, S.; Sporn, M. B. Transforming Growth Factor Alpha: An Aromatic Side Chain at Position 38 Is Essential for Biological Activity. *Mol. Cell. Biol.* **1989**, *9* (2), 860–864.
- (31) Gentzel, M.; Pardo, M.; Subramaniam, S.; Stewart, A. F.; Choudhary, J. S. Proteomic Navigation Using Proximity-Labeling. *Methods* **2019**, *164–165*, 67–72.
- (32) de la Torre, D.; Chin, J. W. Reprogramming the Genetic Code. *Nat. Rev. Genet.* **2021**, *22* (3), 169–184.
- (33) Huang, X.; Luo, X.; Roupioz, Y.; Keillor, J. W. Controlled Regioselective Anilide Formation from Aspartic and Glutamic Acid Anhydrides. *J. Org. Chem.* **1997**, *62* (25), 8821–8825.
- (34) Qin, V. M.; D'Souza, C.; Neeson, P. J.; Zhu, J. J. Chimeric Antigen Receptor beyond CAR-T Cells. *Cancers* **2021**, *13* (3), No. 404.
- (35) Blanc, K. L.; Dazzi, F.; English, K.; Farge, D.; Galipeau, J.; Horwitz, E. M.; Kadri, N.; Krampera, M.; Lalu, M. M.; Nolta, J.; Patel, N. M.; Shi, Y.; Weiss, D. J.; Viswanathan, S. ISCT MSC Committee Statement on the US FDA Approval of Allogenic Bone-Marrow Mesenchymal Stromal Cells. *Cytherapy* **2025**, *27*, 413–416.
- (36) Du, B.; Qin, J.; Lin, B.; Zhang, J.; Li, D.; Liu, M. CAR-T Therapy in Solid Tumors. *Cancer Cell* **2025**, *43* (4), 665–679.
- (37) Tang, L.; Pan, S.; Wei, X.; Xu, X.; Wei, Q. Arming CAR-T Cells with Cytokines and More: Innovations in the Fourth-Generation CAR-T Development. *Mol. Ther.* **2023**, *31* (11), 3146–3162.
- (38) Liu, Y.; Adu-Berchie, K.; Brockman, J. M.; Pezone, M.; Zhang, D. K. Y.; Zhou, J.; Pyrdol, J. W.; Wang, H.; Wucherpfennig, K. W.; Mooney, D. J. Cytokine Conjugation to Enhance T Cell Therapy. *Proc. Natl. Acad. Sci. U.S.A.* **2023**, *120* (1), No. e2213222120.
- (39) Brenner, J. S.; Mitragotri, S.; Muzykantov, V. R. Red Blood Cell Hitchhiking: A Novel Approach for Vascular Delivery of Nano-carriers. *Annu. Rev. Biomed. Eng.* **2021**, *23*, 225–248.
- (40) Armstead, W. M.; Ganguly, K.; Riley, J.; Zaitsev, S.; Cines, D. B.; Higazi, A. A.; Muzykantov, V. R. RBC-Coupled tPA Prevents Whereas tPA Aggravates JNK MAPK-Mediated Impairment of ATP- and Ca-Sensitive K Channel-Mediated Cerebrovasodilation After Cerebral Photothrombosis. *Transl. Stroke Res.* **2012**, *3*, 114–121.
- (41) Secord, E.; Hartog, N. L. Review of Treatment for Adenosine Deaminase Deficiency (ADA) Severe Combined Immunodeficiency (SCID). *Ther. Clin. Risk Manage.* **2022**, *18*, 939–944.
- (42) Levene, M.; Bain, M. D.; Moran, N. F.; Nirmalanathan, N.; Poulton, J.; Scarpelli, M.; Filosto, M.; Mandel, H.; MacKinnon, A. D.; Fairbanks, L.; Pacitti, D.; Bax, B. E. Safety and Efficacy of Erythrocyte Encapsulated Thymidine Phosphorylase in Mitochondrial Neurogastrointestinal Encephalomyopathy. *J. Clin. Med.* **2019**, *8* (4), No. 457.
- (43) Shi, J.; Kundrat, L.; Pishesha, N.; Bilate, A.; Theile, C.; Maruyama, T.; Dougan, S. K.; Ploegh, H. L.; Lodish, H. F. Engineered Red Blood Cells as Carriers for Systemic Delivery of a Wide Array of Functional Probes. *Proc. Natl. Acad. Sci. U.S.A.* **2014**, *111*, 10131–10136.